TRENDS IN SCIENCES 2026; 23(1): 11324
https://doi.org/10.48048/tis.2026.11324 RESEARCH ARTICLE

Bioactive Compounds from *Trentepohlia aurea* as Potential Antibacterial Agents Targeting DNA Gyrase: An *In Vitro* and *In Silico* Approach

Oky Kusuma Atni, Erman Munir* and Nursahara Pasaribu

Department of Biology, Faculty of Mathematics and Natural Sciences, Universitas Sumatera Utara, Medan 20155, North Sumatera, Indonesia

(*Corresponding author's e-mail: erman@usu.ac.id)

Received: 19 July 2025, Revised: 12 August 2025, Accepted: 19 August 2025, Published: 30 October 2025

Abstract

The global rise of antibiotic resistance underscores the urgent need for novel antibacterial agents with new mechanisms of action. *Trentepohlia aurea*, a carotenoid- and phenolic-rich subaerial green alga, remains largely unexplored for its therapeutic potential. This study evaluated the antibacterial activity of its methanol extract via *in vitro* disc diffusion assays and investigated the interaction of its bioactive constituents with bacterial DNA gyrase subunit B (PDB ID: 6KZZ) through *in silico* molecular docking. The extract produced inhibition zones of 11.3 ± 0.55 mm against *Staphylococcus aureus*, 10.9 ± 0.21 mm against *Salmonella Typhii*, and 10.8 ± 0.61 mm against *Streptococcus mutans*, indicating moderate antibacterial activity. GC-MS profiling identified 26 compounds, with Aphthosin exhibiting the strongest predicted gyrase-binding affinity (–7.4 kcal/mol), surpassing a native ligand. ADME-toxicity predictions suggested generally favorable pharmacokinetics with low toxicity, though some compounds displayed organ-specific risks. While MIC/MBC determinations and direct *in vitro* testing of individual compounds were not performed, this first report on *T. aurea* as a potential DNA gyrase inhibitor highlights its promise as a source of structurally diverse natural products for antibacterial drug discovery and warrants further mechanistic validation and potency optimization.

Keywords: Antibacterial, DNA gyrase, GC-MS, *In silico*, Molecular docking, *Trentepohlia aurea*

Introduction

Algae comprise a vast array of photosynthetic organisms, varying from unicellular microscopic species to large multicellular forms, encompassing both prokaryotic and eukaryotic types [1,2]. Algal organisms are prolific producers of structure ally unique and physiologically active compounds. A multitude of alleged bioactive compounds produced by these organisms as primary or secondary metabolites has attracted attention in the pharmaceutical sector [3]. Microalgal metabolism adapts to alterations in the external environment by modifying its internal conditions. Consequently, altering the cultural conditions or the availability of nutrients enhances the synthesis of specific compounds. Several research have been done to explore the products of microalgal metabolism, not only to better understand their nature, but also to look for chemicals with potential human applications in a variety of disciplines. Extracts or metabolites from various microalgae are commonly screened to determine their biological activity. Microalgae have been recognized as abundant suppliers of numerous bio compounds with economic interest [4-6].

The family *Trentepohliaceae* and order *Trentepohliales* include Trentepohlia. The *Ulvophyceae* class of Chlorophyta includes this subaerial algae genus. *Trentepohlia* is the most abundant tropical and subtropical subaerial algae [7]. The diversity of *Trentepohlia* species is influenced by altitude and environmental factors, including humidity, temperature, and light intensity [8]. *Trentepohlia* species synthesize substantial quantities of carotenoids that provide protection against ultraviolet radiation and elevated irradiance. Their pigments give them a distinguishable

yellow, orange, or red color in natural settings [9]. Important bioactive substances identified in the genus *Trentepohlia* include β-carotene, lutein, astaxanthin, microalgal pigments such as chlorophylls (a, b and c), phycocyanin, phycoerythrin, β-carotene, and phycobiliproteins [10]. *Trentepohlia* holds significant potential as a valuable resource in the pharmaceutical sector, particularly for its antimicrobial and antioxidant properties. Its bioactive compounds can be utilized to develop new antimicrobial agents to combat infections and antioxidants to protect against oxidative stress, thereby contributing to advancements in therapeutic and preventive healthcare solutions [11,12].

Schema of the PDB The DNA gyrase B complex with a 2-oxo-1,2-dihydroquinoline derivative is seen in the crystal structure of *Escherichia coli* at 6KZZ. One of the most important enzymes for DNA replication and transcription is DNA gyrase, which is produced by bacteria. It adds negative supercoils into DNA [13]. The 2 components of DNA gyrase, GyrA and GyrB, work together as a heterodimer. DNA cleavage and rejoining are carried out by GyrA, whereas the energy required for these processes is supplied by GyrB, which displays ATPase activity [14,15]. The GyrB subunit is targeted by many antibacterial agents due to its role in ATP hydrolysis. Competing in ATP GyrB inhibitors are made up of different chemical groups, such as coumarins, arylaminopyrimidines, ethyl ureas, tricyclic inhibitors, and pyrrolamides. They are good at killing both Gram-positive and Gram-negative bacteria [16]. The 6KZZ structure provides significant insights into the binding interactions and mechanisms of these inhibitors. Comprehending this structural information is essential for clarifying the impact of these compounds on DNA gyrase function, thereby facilitating the creation of novel antimicrobial agents and strategies to address bacterial resistance. Remarkably, metabolites derived from algae, such as those from *T. aurea,* have demonstrated the ability to inhibit DNA gyrase similarly to synthetic antibiotics. This provides new ways to improve treatment efficacy against resistant bacterial strains and emphasizes the possibility of chemicals derived from algae as natural alternatives to tackle the increasing problem of bacterial resistance.

Materials and methods

Preparation of the *Trentepohlia aurea* extracts

Trentepohlia aurea (Linnaeus) C. Martius, obtained from Bukit Barisan Grand Forest Park, North Sumatra, Indonesia, was initially cleaned and desiccated. The samples were desiccated in an oven (UN 55 Universal Oven, Memmert, Germany) at 35 °C for 4 - 5 days to eliminate residual moisture. The desiccated algal substance was subsequently pulverized into a fine powder utilizing a blender. Extraction was conducted via the maceration method utilizing 70% methanol for 3 successive cycles, each lasting 24 h, at ambient temperature on a shaker operating at 150 rpm. Following each cycle, the filtrate was extracted from the residue utilizing filter paper. The amalgamated filtrates were concentrated with a rotary evaporator to yield a viscous extract. Using Dimethyl Sulfoxide (DMSO) as the solvent, the concentrated extract was further diluted until it reached a final concentration of 50%. The crude extract yield was 2.78 g, corresponding to 2.78 %(w/w) of the initial dry biomass. No standardization or quantification of total phenolic, flavonoid, or carotenoid content was performed in this study, which is acknowledged as a limitation in interpreting the bioactivity results.

Antibacterial assays of *Trentepohlia aurea* extracts

Pathogens used for antibacterial activity

In this study, we employed 3 Gram-positive bacterial strains: *Staphylococcus aureus* ATCC 6538, *Propionibacterium acnes* ATCC 6919, and *Streptococcus mutans* ATCC 35668, alongside 3 Gram-negative strains: *Salmonella enterica* serovar Typhii IPBCC b 11 669, *Escherichia coli* ATCC 8739, and *Pseudomonas aeruginosa* ATCC 15442, to evaluate their antimicrobial activity.

Antibacterial activity

The evaluation of antibacterial efficacy was conducted using the disc diffusion method [17-19]. Twenty mL of Mueller-Hinton Agar (MHA) medium was dispensed into sterile Petri dishes and allowed to solidify. A bacterial suspension, adjusted to the turbidity of a 0.5 McFarland standard, was uniformly spread across the agar surface using a sterile cotton swab. Sterile 6 mm discs were impregnated with 100 µL of a

50% methanolic extract of *T. aurea* and placed onto the inoculated agar. Chloramphenicol served as the positive control and dimethyl sulfoxide (DMSO) as the negative control. The plates were incubated at room temperature for 24 h, and antibacterial activity was determined by measuring the inhibition zone diameters.

GC-MS analysis

A 1 µL volume of the filtered sample, obtained via a membrane filter, was injected into a Shimadzu GCMS-QP2010 Plus for volatile component profiling. Prior to injection, the crude 70% methanol extract obtained by maceration was concentrated and diluted using 2 mL of HPLC-grade methanol (99.5%). No derivatization was performed. The prepared sample was injected using a split ratio of 1:1 through a split-splitless injector maintained at 250 °C, with the mass spectrometer detector temperature set at 280 °C. Separation was achieved on a Restek Rtx®-50 column (Crossbond® 5% phenyl-50% methyl polysiloxane, 30 m×0.25 mm i.d., 0.25 µm film thickness). Helium was used as the carrier gas at 64.1 kPa, with a total flow of 4.9 mL/min, column flow of 0.99 mL/min, linear velocity of 36.6 cm/s, and purge flow of 3.0 mL/min. The oven temperature was programmed from 80 °C (held for 2 min) to 280 °C (held for 8 min). Peak identification was performed using the Wiley9.LIB and cross-validated with the NIST17 library, with a minimum similarity index (SI) threshold of 70 - 80 to confirm compound matches. Compound assignments were based on an internal method following established GC-MS identification criteria. Although the analysis was conducted on a crude methanol extract without preliminary fractionation, this approach was selected to capture the full spectrum of volatile and semi-volatile constituents present in the extract, in line with previous studies reporting reliable bioactive compound detection under similar conditions [18,19].

Protein-ligan preparation

The bioactive compounds from *T. aurea* used in this study are: Here is a paragraph that includes the compound names with their respective PubChem IDs: Morpholine, 2,6-dimethyl-4-tridecyl- (32518), Carbamic acid, monoammonium salt (517232), Oxiranemethanol (11164), Hexanal (6184), Heptanal (8130), Dianhydroglucitol, tbs 2x, Cyclohexanone, 2,2,6-trimethyl- (17000), 2 octenal (5283324), Cyclopentanone, 2-methyl-3-(1-methylethyl)- (41124), 1-methylcycloheptanol (77376), 1,2,3-propanetriol (753), 2-decenal, (e)- (5283345), 6-methyl-6-nitro-2-heptanone (537587), Isosorbide (12597), (2,2,6,6-tetramethylcyclohexylidene) methanone, 2-Benzofuranmethanol, 2,4,5,6,7,7a-hexahydro-4,4,7a-trimethyl-, cis- (21578471), Phenol, 2,6-dimethoxy- (7041), Trans-. Beta. -ionon-5,6-epoxide, 8-hydroxygeraniol (5363397), 2(4H)-Benzofuranone, 5,6,7,7a-tetrahydro-4,4,7a-trimethyl- (27209), 1,2,3,4-tetrahydroxybutane (8998), Tetradecanoic acid (11005), Hexadecanoic acid, methyl ester (8181), Aphthosin (15595748), Hexadecanoic acid (985), 10,13-Eicosadienoic acid, methyl ester (5365687). Furthermore, the compound 4-[[8-(methylamino)-2-oxidanylidene-1~{H}-quinolin-3-yl]carbonylamino]benzoic acid9 (Control) (PubChem CID:) was employed as a reference control chemical to evaluate the inhibitory properties of the bioactive compounds obtained from *T. aurea*. The 2D and 3D structures of the active ingredients found in *T. aurea* and the control were acquired from the appropriate chemical databases on PubChem. Subsequently, these structures were optimized for energy and transformed into the .pdb file format using Open Babel in PyRx software.

Biological activities prediction using the PASS online

The biological activity prediction of the bioactive compounds from *T. aurea* was performed using the Prediction of Activity Spectra for Substances (PASS) server on the Way2drug platform (http://way2drug.com/PassOnline/). The SMILES structures of each GC-MS-identified compound were retrieved from the PubChem database (http://pubchem.ncbi.nlm.nih.gov) and submitted individually to the PASS Online server. The prediction results provided probability of activity (Pa) and inactivity (Pi) values for various biological functions. In this study, a Pa value > 0.70 was considered to indicate high potential biological activity, $0.50 \leq Pa \leq 0.70$ indicated moderate activity, and $Pa < 0.50$ suggested low activity. Twenty-two compounds with available SMILES data were evaluated, with details presented in **Table 2**. The combination of high Pa values and low Pi

values was used to prioritize compounds for further docking and ADME-toxicity analyses.

Prediction drug-likeness

Lipinski's rule of 5 was utilized to assess the degree to which the compounds mimicked the properties of drugs. All the compounds were evaluated using SwissADME (http://www.swissadme.ch/), which is a drug-likeness evaluation framework. The number of hydrogen bond acceptors and donors, the molecular weight, and the bioavailability of the molecule are some of the parameters that are included in this resource. It is possible to determine the oral bioavailability of a compound with the help of Lipinski's rule of 5.

Pharmacokinetics predictions

Pharmacokinetics predictions were evaluated by assessing each compound's ability to penetrate the blood-brain barrier (BBB) using the pkcSM webserver (http://biosig.lab.uq.edu.au/pkcsm/prediction). Additionally, both BBB permeability and human intestinal absorption (HIA) patterns were analyzed using the BOILED-Egg predictive model.

Molecular docking analysis

Molecular docking was performed to evaluate the binding affinities of the identified compounds toward DNA Gyrase subunit B (PDB ID: 6KZZ). Protein and ligand preparations were conducted using BIOVIA Discovery Studio 2024 for visualization, removal of water molecules and co-crystallized ligands, and the addition of polar hydrogen atoms when necessary. Ligand structures were retrieved from the PubChem database (http://pubchem.ncbi.nlm.nih.gov) in *.sdf* format, optimized, and converted into *.pdbqt* format using Open Babel integrated in PyRx v.0.8. DNA Gyrase was selected as it plays a crucial role in bacterial DNA replication and is a well-established target for antibacterial drug development.

Docking simulations were carried out using AutoDock Vina within PyRx 8.0.0, treating the protein as the macromolecule and the bioactive compounds as ligands. The docking grid box was set with center coordinates at (1.3057×1.4901×0.3121) and dimensions of (36.7569×19.5379×18.1727 $Å^3$) to encompass the active site. Binding affinity values (kcal/mol) were used to rank ligand–protein interactions, and the interaction profiles were analyzed to identify hydrogen bonds, hydrophobic interactions, and electrostatic contacts. Visualization and identification of key amino acid residues at the binding site were performed using both PyMOL and BIOVIA Discovery Studio 2024.

Results and discussion

***T. aurea* morphology**

T. aurea, a terrestrial filamentous green alga gathered in Bukit Barisan Grand Forest Park, North Sumatra, Indonesia, as illustrated in **Figure 1**, is a cosmopolitan species with an extensive distribution range. This wide distribution highlights its strong ecological adaptability and ability to occupy diverse ecological niche.

Trentepohlia aurea (L.) C.F.P. Martius, Family: Ulvophyceae. Filamentous form: Fine filaments growing upright in very large numbers, capable of covering extensive surfaces in golden-yellow, yellow-orange, and orange colors. Habitat: Humid, shaded environments, adhering to tree bark, rocks, and moist cement walls. Distribution: Widespread throughout the study area at altitudes ranging from 867 to 978 masl. Characterized by carotenoid pigments that mask green chlorophyll and contribute to its striking yellow-orange coloration. This green alga often symbiotically associates with lichenized fungi, acting as a photobiont in such cases. Identification was based solely on morphological characteristics following relevant taxonomic keys, without voucher specimen deposition or molecular confirmation, which is acknowledged as a limitation given the morphological similarity among members of the order *Trentepohliales*.

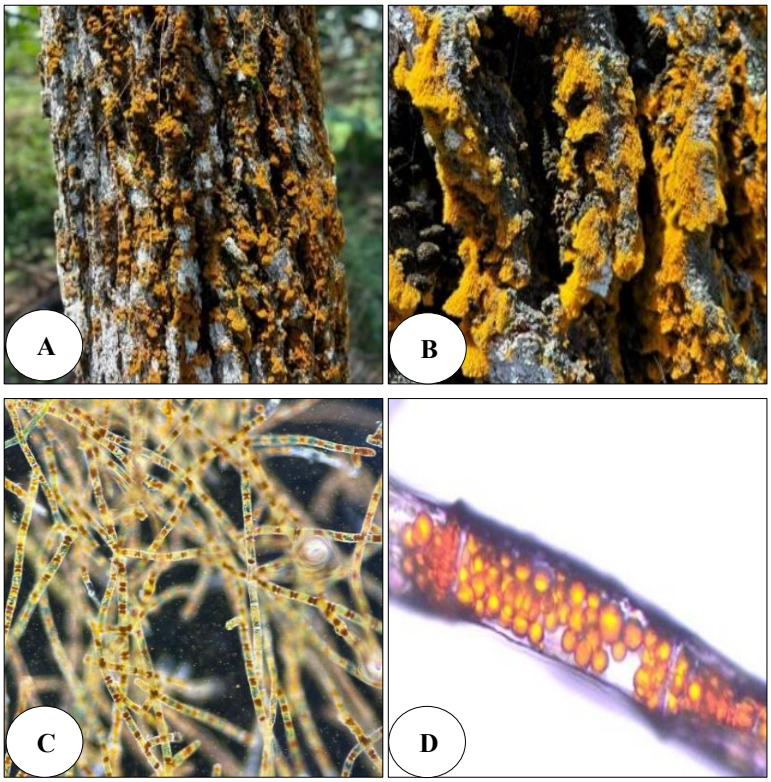

Figure 1 Morphology of *T. aurea*: (A) Trees covered with massive growth of *T. aurea*; (B) Population of *T. aurea* on the tree bark; (C) *T. aurea* filaments observed under 100× magnification; (D) Carotenoid pigments in *T. aurea* filaments observed under 400× magnification. (C) and (D) were captured using an Olympus CX43 microscope equipped with a DP75 camera and CellSens Dimensions software.

Antimicrobial activity *Trentepohlia aurea*

The subsequent table displays the outcomes of antimicrobial activity assays utilizing methanol extracts of *T. aurea*, assessed against various pathogenic microorganisms. Chloramphenicol (10 µg/disk) was used as a standard antibiotic positive control, and DMSO as a negative control, to enable comparison of the extract's relative efficacy. **Table 1** presents the results of antimicrobial activity testing utilizing methanol extract from *T. aurea* algae against diverse pathogenic microorganisms. The highest activity is observed against *S. aureus*, a Gram-positive bacterium, with an inhibition zone 11.3 ± 0.55 mm. Additionally, the methanol extract also exhibits significant antimicrobial activity against *S. enterica* serovar Typhii 10.9 ± 0.21 mm (**Figure 2**) and *S. mutans* 10.8 ± 0.61 mm. However, lower activity is observed against *E. coli* and *P. aeruginosa* with inhibition zone 10.0 ± 1.22 mm and 9.8 ± 0.70 mm, respectively. The data suggest that the methanol extract from *T. aurea* possesses potential as an antimicrobial agent against various bacteria, particularly exhibiting the highest efficacy against Gram-positive bacteria like *S. aureus*.

Table 1 Antimicrobial efficacy of methanol extract from aerial microalgae *T. aurea.*

Microorganism		Inhibition zone (mm)	
		Methanol extract algae (10 µL/disk)	**Chloramphenicol**
Gram-Negative Bacteria	*S. enterica* serovar Typhii IPBCC b 11 669	10.9 ± 0.21	25.2 ± 0.5
	E. coli ATCC 8739	10.0 ± 1.22	24.9 ± 1.7
	P. aeruginosa ATCC 15442	9.8 ± 0.70	28.7 ± 1.8
	S. aureus ATCC 6538	11.3 ± 0.55	31.1 ± 1.5

	Microorganism	Inhibition zone (mm)	
		Methanol extract algae (10 µL/disk)	Chloramphenicol
Gram-Positive Bacteria	*P. acnes* ATCC 6919	-	14.8 ± 1.0
	S. mutans ATCC 35668	10.8 ± 0.61	27.1 ± 0.4

The green alga *Trentepohlia umbrina* has been previously studied for antimicrobial activity by Simic *et al.* [20], whereas studies on the antimicrobial activity of *T. aurea* are currently being investigated for the first time. Consistent with results from studies on other algae, we observed that the methanol extract of *T. aurea* exhibited relatively strong antimicrobial activity, more so than Gram-negative bacteria, especially when it comes to Gram-positive bacteria. These differences in antimicrobial activity are attributed to variations in the cell walls of both gram-positive and gram-negative bacteria. Gram-negative bacteria feature 2 lipid membranes with peptidoglycan and lipopolysaccharides (LPS), along with a periplasmic space containing degrading enzymes [21]. The cell walls of Gram-positive bacteria are thick and made of cross-linked peptidoglycan. They also have a single lipid membrane. The structural differences between Gram-positive and Gram-negative bacteria explain why antibacterial agents are more effective against the former [22].

In addition, carotenoids, including β-carotene, are key compounds found in *T. aurea*, contributing to its hues ranging from golden-yellow to orange tones [23]. Although research on the antibacterial properties of microalgal β-carotene is limited, recent findings by Jaber and Majeed [24], highlight its potent β-carotene antibacterial activity against various bacteria, particularly Gram-positive strains. These results emphasize β-carotene's potential as a promising antimicrobial agent.

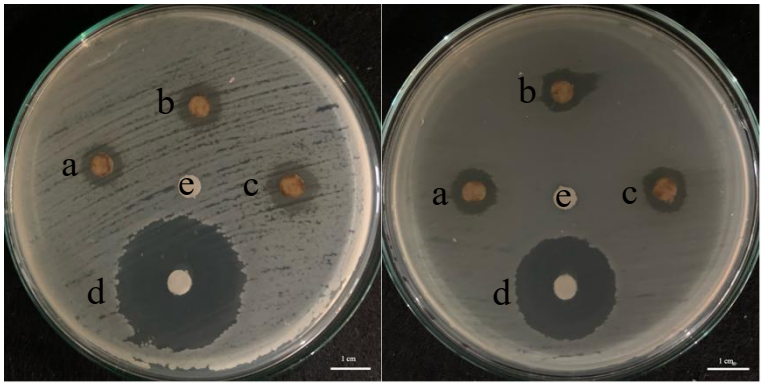

Figure 2 Inhibition zones of methanol extract of *T. aurea* against bacteria: (A) Gram-positive bacteria *S. aureus* (a) - (c). Replicates of methanol extract of *T. aurea*; (d) Positive control (Chloramphenicol); (e) Negative control (Dimethyl sulfoxide)), and (B) Gram-negative bacteria *S. enterica* serovar Typhii (a) - (c). Replicates of methanol extract of *T. aurea*; (d) Positive control (Chloramphenicol); (e) Negative control (Dimethyl sulfoxide).

Gas chromatograpy-mass spectrometry analysis

Raw data from GC-MS and individual chromatograms were processed using Origin software. The GC-MS analysis revealed 26 bioactive compounds in *T. aurea.* These compounds include Morpholine, 2,6-dimethyl-4-tridecyl-, Carbamic acid, monoammonium salt, Oxiranemethanol, Hexanal, Heptanal, Dianhydroglucitol, tbs 2x, Cyclohexanone, 2,2,6-trimethyl-, 2 octenal, Cyclopentanone, 2-methyl-3-(1-methylethyl)-, 1-methylcycloheptanol, 1,2,3-propanetriol, 2-decenal, (e)-, 6-methyl-6-nitro-2-heptanone, Isosorbide, (2,2,6,6-tetramethylcyclohexylidene) methanone, 2-Benzofuranmethanol, 2,4,5,6,7,7a-hexahydro-4,4,7a-trimethyl-, cis-, Phenol, 2,6-dimethoxy-, Trans-. Beta. -

ionon-5,6-epoxide, 8-hydroxygeraniol, 2(4H)-Benzofuranone, 5,6,7,7a-tetrahydro-4,4,7a-trimethyl-, 1,2,3,4-tetrahydroxybutane, Tetradecanoic acid, Hexadecanoic acid, methyl ester, Aphthosin, Hexadecanoic acid, 10,13-Eicosadienoic acid, methyl ester. Retention times are presented in **Table 2**, and the chromatogram is depicted in **Figure 3**. Based on a screening in PubChem, certain compounds do not possess available 3D structures; therefore, 22 of these compounds catalogued in the database will be employed for docking analysis.

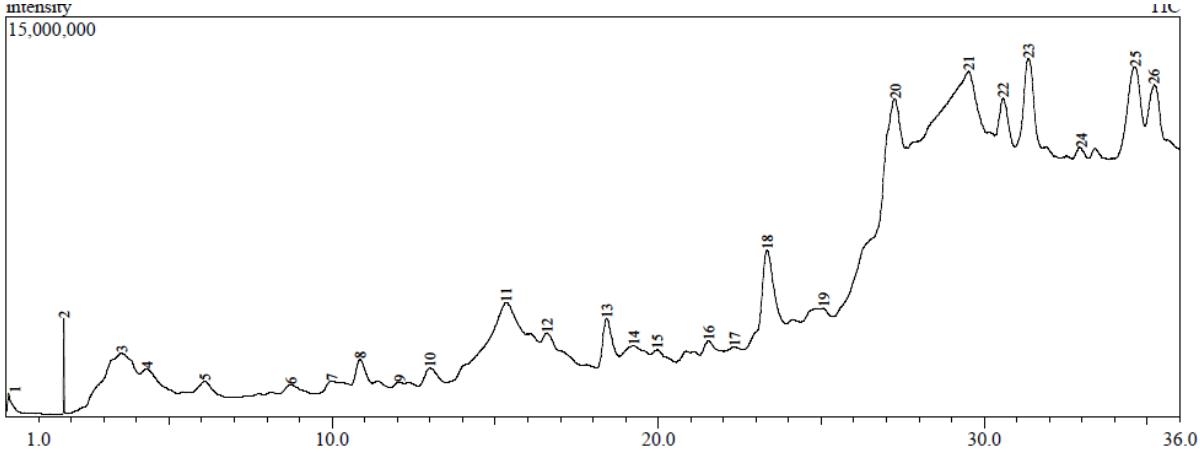

Figure 3 GC-MS Chromatogram of *T. Aurea*.

Table 2 Compounds of *T. aurea* (linnaeus) *C. martius*.

No	Compound name	Mol. Formula	Mass (g/mol)	R. Time (min)	Smiles	PubChem CID
1	Morpholine, 2,6-dimethyl-4-tridecyl-	$C_{19}H_{39}NO$	297	0.076	CCCCCCCCCCCCCN1CC(OC(C1)C)C	32518
2	Carbamic acid, monoammonium salt	CH_3NO_2	61	1.775	C(=O)(N)[O^-]·[NH^{4+}]	517232
3	Oxiranemethanol	$C_3H_6O_2$	74	3.548	C1C(O1)CO	11164
4	Hexanal	$C_6H_{12}O$	100	4.325	CCCCCC=O	6184
5	Heptanal	$C_7H_{14}O$	114	6.104	CCCCCCC=O	8130
6	Dianhydroglucitol, tbs 2x	$C_{12}H_{24}O_2$	200	8.742		
7	Cyclohexanone, 2,2,6-trimethyl-	$C_9H_{16}O$	140	9.99	CC1CCCC(C1=O)(C)C	17000
8	2 octenal	$C_8H_{14}O$	126	10.864	CCCCCC=CC=O	5283324
9	Cyclopentanone, 2-methyl-3-(1-methylethyl)-	$C_9H_{16}O$	140	2.083	CC1C(CCC1=O)C(C)C	41124
10	1-methylcycloheptanol	$C_8H_{16}O$	128	3.002	CC1(CCCCCC1)O	77376
11	1,2,3-propanetriol	$C_3H_8O_3$	92	15.341	C(C(CO)O)O	753
12	2-decenal, (e)-	$C_{10}H_{18}O$	154	16.598	CCCCCCCC=CC=O	5283345
13	6-methyl-6-nitro-2-heptanone	$C_8H_{15}NO_3$	173	18.432	CC(=O)CCCC(C)(C)[N^+](=O)[O^-]	537587
14	Isosorbide	$C_6H_{10}O_4$	146	19.256	C1C(C2C(O1)C(CO2)O)O	12597
15	(2,2,6,6-tetramethylcyclohexylidene) methanone	$C_{11}H_{18}O$	166	19.976		349282968

No	Compound name	Mol. Formula	Mass (g/mol)	R. Time (min)	Smiles	PubChem CID
16	2-Benzofuranmethanol, 2,4,5,6,7,7a-hexahydro-4,4,7a-trimethyl-, cis-	$C_{12}H_{20}O_2$	196	21.554	CC1(CCCC2(C1=CC(O2)CO)C)C	21578471
17	Phenol, 2,6-dimethoxy-	$C_8H_{10}O_3$	154	22.342	COC1=C(C(=CC=C1)OC)O	7041
18	Trans-. Beta. -ionon-5,6-epoxide	$C_{13}H_{20}O_2$	208	23.345		
19	8-hydroxygeraniol	$C_{10}H_{18}O_2$	170	25.081	CC(=CCO)CCC=C(C)CO	5363397
20	2(4H)-Benzofuranone, 5,6,7,7a-tetrahydro-4,4,7a-trimethyl-	$C_{11}H_{16}O_2$	180	27.275	CC1(CCCC2(C1=CC(=O)O2)C)C	27209
21	1,2,3,4-tetrahydroxybutane	$C_4H_{10}O_4$	122	29.523	C(C(C(CO)O)O)O	8998
22	Tetradecanoic acid	$C_{14}H_{28}O_2$	228	30.578	CCCCCCCCCCCCCC(=O)O	11005
23	Hexadecanoic acid, methyl ester	$C_{17}H_{34}O_2$	270	31.353	CCCCCCCCCCCCCCCC(=O)OC	8181
24	Aphthosin	$C_{34}H_{30}O_{13}$	646	32.984	CC1=CC(=CC(=C1C(=O)OC2=CC(=C(C(=C2)C)C(=O)OC3=CC(=C(C(=C3)C)C(=O)OC4=CC(=C(C(=C4)C)C(=O)OC)O)O)O)O)OC	15595748
25	Hexadecanoic acid	$C_{16}H_{32}O_2$	256	34.633	CCCCCCCCCCCCCCCC(=O)O	985
26	10,13-Eicosadienoic acid, methyl ester	$C_{21}H_{38}O_2$	322	35.202	CCCCCCC=CCC=CCCCCCCCCC(=O)OC	5365687

Prediction of compound biological activities

The predicted antimicrobial potential of various compounds from *T. aurea*, based on their inhibition of key microbial targets, is presented in **Table 3**. For instance, Morpholine, 2,6-dimethyl-4-tridecyl- shows high activity as a membrane integrity antagonist (Pa = 0.886, Pi = 0.003) and sphinganine kinase inhibitor (Pa = 0.789, Pi = 0.015), both of which can disrupt microbial cell functions. Oxiranemethanol exhibits relatively strong inhibitory potential against glucan endo-1,3-beta-D-glucosidase (Pa = 0.940, Pi = 0.002) and saccharopepsin (Pa = 0.960, Pi = 0.002), which are crucial for microbial cell wall and protein synthesis. Tetradecanoic acid has high inhibitory activity against saccharopepsin (Pa = 0.961, Pi = 0.002) and glucan endo-1,3-beta-D-glucosidase (Pa = 0.945, Pi = 0.002). Similarly, Hexadecanoic acid, methyl ester shows relatively strong potential as a saccharopepsin inhibitor (Pa = 0.962, Pi = 0.002) and chymosin inhibitor (Pa = 0.962, Pi = 0.002). Heptanal is predicted to inhibit exoribonuclease II (Pa = 0.846, Pi = 0.004) and chymosin (Pa = 0.909, Pi = 0.004), while 2-Decenal, (E)- is shown to be an antieczematic agent (Pa = 0.903, Pi = 0.005) and TRPA1 agonist (Pa = 0.705, Pi = 0.002), potentially disrupting microbial integrity. The elevated Pa and diminished Pi values suggest a significant probability of antimicrobial effectiveness, rendering these compounds viable candidates for additional investigation in antimicrobial drug development.

Table 3 Prediction biological activity compounds of *T. aurea*.

No	Compound name	Biological activity	Pa	Pi	Criteria
1	Morpholine, 2,6-dimethyl-4-tridecyl- (CAS)	Membrane integrity antagonist	0.886	0.003	High
		Polyporopepsin inhibitor	0.789	0.022	High
		Sphinganine kinase inhibitor	0.789	0.015	High
2	Carbamic acid, monoammonium salt (CAS)	-	-	-	-

No	Compound name	Biological activity	Pa	Pi	Criteria
3	Oxiranemethanol (CAS)	Glucan endo-1,3-beta-D-glucosidase inhibitor	0.940	0.002	High
		Alkenylglycerophosphocholine hydrolase inhibitor	0.924	0.004	High
		Saccharopepsin inhibitor	0.960	0.002	High
		Polyporopepsin inhibitor	0.939	0.003	High
4	Hexanal (CAS)	Glucan 1,4-alpha-maltotriohydrolase inhibitor	0.880	0.002	High
		Cyclomaltodextrinase inhibitor	0.891	0.002	High
		Antiseptic	0.718	0.005	High
		Alkenylglycerophosphocholine hydrolase inhibitor	0.876	0.008	High
5	Heptanal (CAS)	Exoribonuclease II inhibitor	0.846	0.004	High
		Chymosin inhibitor	0.909	0.004	High
		Polyporopepsin inhibitor	0.940	0.003	High
		Acrocylindropepsin inhibitor	0.909	0.004	High
6	Cyclohexanone, 2,2,6-trimethyl- (CAS)	Antieczematic	0.788	0.021	High
		Membrane permeability inhibitor	0.705	0.037	
		Antiseborrheic	0.760	0.026	High
7	2 OCTENAL	Chymosin inhibitor	0.866	0.009	High
		Saccharopepsin inhibitor	0.866	0.009	High
		Cutinase inhibitor	0.810	0.005	High
		Fusarinine-C ornithinesterase inhibitor	0.700	0.023	High
8	Cyclopentanone, 2-methyl-3-(1-methylethyl)- (CAS)	Antieczematic	0.887	0.005	High
		Membrane permeability inhibitor	0.774	0.015	High
		Antiseborrheic	0.704	0.037	High
9	1-Methylcycloheptanol	Membrane integrity agonist	0.903	0.010	High
		Antiseborrheic	0.884	0.005	High
		NADPH peroxidase inhibitor	0.787	0.014	High
10	1,2,3-Propanetriol (CAS)	Membrane integrity agonist	0.945	0.004	High
		Saccharopepsin inhibitor	0.915	0.004	High
		Chymosin inhibitor	0.915	0.004	High
11	2-Decenal, (E)- (CAS)	Glutamyl endopeptidase II inhibitor	0.720	0.023	High
		TRPA1 agonist	0.705	0.002	High
		Antieczematic	0.903	0.005	High
12	6-methyl-6-nitro-2-heptanone	Gluconate 2-dehydrogenase (acceptor) inhibitor	0.933	0.003	High
		Saccharopepsin inhibitor	0.861	0.010	High
		Acrocylindropepsin inhibitor	0.861	0.010	High
		Chymosin inhibitor	0.861	0.010	High
13	Isosorbide	Pectate Lyase Inhibitor	0.700	0.005	High

No	Compound name	Biological activity	Pa	Pi	Criteria
		Polyporopepsin inhibitor	0.756	0.028	High
		Manganese peroxidase inhibitor	0.789	0.005	High
14	2-Benzofuranmethanol, 2,4,5,6,7,7a-hexahydro-4,4,7a-trimethyl-, cis- (CAS)	Antieczematic	0.748	0.031	High
		Glucan endo-1,6-beta-glucosidase inhibitor	0.731	0.015	High
		UDP-N-acetylglucosamine 4-epimerase inhibitor	0.710	0.015	High
15	Phenol, 2,6-dimethoxy- (CAS)	Membrane integrity agonist	0.901	0.011	High
		Antiseborrheic	0.876	0.006	High
		Saccharopepsin inhibitor	0.850	0.011	High
		Acrocylindropepsin inhibitor	0.850	0.011	High
16	8-hydroxygeraniol	Retinol dehydrogenase inhibitor	0.940	0.000	High
		Undecaprenyl-phosphate mannosyltransferase inhibitor	0.938	0.001	High
		Membrane integrity agonist	0.793	0.038	High
17	2(4H)-Benzofuranone, 5,6,7,7a-tetrahydro-4,4,7a-trimethyl- (CAS)	General pump inhibitor	0.744	0.005	High
		CYP2J substrate	0.807	0.019	High
		Antieczematic	0.791	0.020	High
18	1,2,3,4-Tetrahydroxybutane	Macrophage stimulant	0.926	0.001	High
		Beta-mannosidase inhibitor	0.927	0.001	High
		Mannose isomerase inhibitor	0.826	0.001	High
19	Tetradecanoic acid (CAS)	Acrocylindropepsin inhibitor	0.961	0.002	High
		Saccharopepsin inhibitor	0.961	0.002	High
		Glucan endo-1,3-beta-D-glucosidase inhibitor	0.945	0.002	High
20	Hexadecanoic acid, methyl ester (CAS)	Saccharopepsin inhibitor	0.962	0.002	High
		Acrocylindropepsin inhibitor	0.942	0.003	High
		Chymosin inhibitor	0.962	0.002	High
		Acylcarnitine hydrolase inhibitor	0.942	0.003	High
21	Aphthosin	Antiseptic	0.852	0.004	High
		Antifungal	0.500	0.030	Low
		Membrane integrity agonist	0.881	0.016	High
22	Hexadecanoic acid (CAS)	Saccharopepsin inhibitor	0.961	0.002	High
		Chymosin inhibitor	0.961	0.002	High
		CYP2J substrate	0.962	0.002	High
		Acrocylindropepsin inhibitor	0.961	0.002	High

Prediction of drug-likeness

According to Lipinski's rule of 5, which assesses a compound's drug-likeness based on molecular weight (MW ≤ 500), lipophilicity (MlogP ≤ 4.15), number of hydrogen bond donors (NHorOH ≤ 5), and acceptors (NorO ≤ 10), **Table 4** lists the physicochemical properties of different compounds from *T. aurea*. Compounds like Carbamic acid, monoammonium salt (MW = 61, MlogP = −6.14, 0 violations), Oxiranemethanol (MW = 74, MlogP = −1.03, 0

violations), Hexanal (MW = 100, MlogP = 1.39, 0 violations), Heptanal (MW = 114, MlogP = 1.74, 0 violations), and 1,2,3-Propanetriol (MW = 92, MlogP = −1.51, 0 violations) show no violations, indicating good drug-like properties and potential oral bioavailability. Others, such as Hexadecanoic acid, methyl ester (MW = 270, MlogP = 4.44, 1 violation) and Hexadecanoic acid (MW = 256, MlogP = 4.19, 1 violation) have slightly higher lipophilicity, leading to one violation, which could affect their absorption or permeability. Aphthosin (MW = 646, MlogP = 2.83, 2 violations) has a high molecular weight and multiple hydrogen bond acceptors, suggesting it may have poor absorption and limited oral bioavailability. Overall, most compounds adhere to Lipinski's criteria, indicating favorable pharmacokinetic properties, making them promising candidates for further drug development research.

To estimate the likelihood that a chemical molecule with a given pharmacological or biological action will have an oral effect on humans, the Rule of Five (ROF) is used as a general guideline [25]. The ROF rating for an orally active medicine ranges from "0" to "4", indicating no more than one violation of the exposed criterion. Lipinski cautions against dismissing these molecules entirely, as many medicines do not undergo ROF [26]. Although the rule of 5 has a broad application, there are certain flaws. The 2 key drawbacks are the equal weight given to each rule and the sharp boundary that signals a breach of a specific rule. Another problem of this approach is that it does not consider natural and biological compounds. ROF excludes metabolic-related criteria.

Table 4 Physicochemical properties of compounds from *T. aurea*.

No	Compound name	Lipinski				
		MW	**MlogP ≤ 4.15**	**NorO ≤ 10**	**NHorOH ≤ 5**	**Violasi**
1	Morpholine, 2,6-dimethyl-4-tridecyl-	297	3.85	2	0	Yes (0)
2	Carbamic acid, monoammonium salt	61	−6.14	2	2	Yes (0)
3	Oxiranemethanol	74	−1.03	2	1	Yes (0)
4	Hexanal	100	1.39	1	0	Yes (0)
5	Heptanal	114	1.74	1	0	Yes (0)
6	Cyclohexanone, 2,2,6-trimethyl-	140	2	1	0	Yes (0)
7	2 octenal	126	1.97	1	0	Yes (0)
8	Cyclopentanone, 2-methyl-3-(1-methylethyl)-	140	2	1	0	Yes (0)
9	1-methylcycloheptanol	128	1.83	1	1	Yes (0)
10	1,2,3-propanetriol	92	−1.51	3	3	Yes (0)
11	2-decenal, (e)-	154	2.59	1	0	Yes (0)
12	6-methyl-6-nitro-2-heptanone	173	0.59	3	0	Yes (0)
13	Isosorbide	146	−1.52	4	2	Yes (0)
14	2-Benzofuranmethanol, 2,4,5,6,7,7a-hexahydro-4,4,7a-trimethyl-, cis-	196	1.95	2	1	Yes (0)
15	Phenol, 2,6-dimethoxy-	154	0.87	3	1	Yes (0)
16	8-hydroxygeraniol	170	1.66	2	2	Yes (0)
17	2(4H)-Benzofuranone, 5,6,7,7a-tetrahydro-4,4,7a-trimethyl-	180	2.37	2	0	Yes (0)
18	1,2,3,4-tetrahydroxybutane	122	−1.91	4	4	Yes (0)
19	Tetradecanoic acid	228	3.69	2	1	Yes (0)
20	Hexadecanoic acid, methyl ester	270	4.44	2	0	Yes (1)

No	Compound name	Lipinski				
		MW	MlogP ≤ 4.15	NorO ≤ 10	NHorOH ≤ 5	Violasi
21	Aphthosin	646	2.83	13	4	No (2)
22	Hexadecanoic acid	256	4.19	2	1	Yes (1)

Pharmacokinetics prediction

The pharmacokinetic evaluation of *T. aurea* compounds, shown in **Table 5**, reveals diverse absorption, distribution, and metabolic characteristics. HIA rates range from 51.7% to 97.5%, with most compounds exceeding 90%, indicating efficient gastrointestinal absorption. Caco-2 permeability values for all compounds are greater than 1, suggesting effective traversal of the intestinal epithelial barrier, a critical factor for oral bioavailability. Among the compounds, Morpholine, 2,6-dimethyl-4-tridecyl-, stands out as both a substrate and inhibitor of the CYP2D6 enzyme and interacts with the OCT2 transporter, hinting at potential metabolic and renal transport complexities. In contrast, most compounds, including Hexanal, Heptanal, and Cyclopentanone derivatives, do not exhibit CYP2D6 or OCT2 interactions, suggesting stable metabolic and renal profiles. Water solubility varies significantly, with compounds like Oxiranemethanol and 1,2,3-propanetriol demonstrating high solubility, supporting their absorption. Conversely, lipophilic compounds such as Hexadecanoic acid and its methyl ester exhibit poor solubility (log mol/L < −6), which may influence their bioavailability despite favorable absorption rates. BBB permeability analysis reveals that most compounds, such as Hexadecanoic acid and its methyl ester, possess moderate to high permeability (log BB values between 0.5 and 0.7), indicating their potential to reach the central nervous system (CNS). Compounds like Carbamic acid, monoammonium salt, show limited BBB penetration (log BB < 0), restricting their CNS access. These findings highlight the varied pharmacokinetic potential of *T. aurea* compounds, with most demonstrating effective gastrointestinal absorption, some capable of CNS permeation, and others maintaining metabolic stability. This diversity suggests promising applications for these compounds in pharmacological development.

Table 5 Pharmacokinetic characteristics of compounds from *T. Aurea*.

No	Compound name	Water solubility (log mol/L)	Human intesntinal absorption (% Absorbed)	Caco-2 permeability (log Papp in 10^{-6} cm/s)	BBB permeability (log BB)	CYP2D6 substrate	CYP2D6 inhibitor	OCT2 substrate
1	Morpholine, 2,6-dimethyl-4-tridecyl-	−5.802	89.774	1.48	0.864	Yes	Yes	Yes
2	Carbamic acid, monoammonium salt	−2.738	51.699	−0.359	−0.132	No	No	No
3	Oxiranemethanol	0.689	97.231	1.569	−0.255	No	No	No
4	Hexanal	−1.758	95.788	1.488	0.512	No	No	No
5	Heptanal	−2.406	95.432	1.487	0.546	No	No	No
6	Cyclohexanone, 2,2,6-trimethyl-	−2.122	96.981	1.508	0.267	No	No	No
7	2 octenal	−2.84	95.588	1.493	0.658	No	No	No
8	Cyclopentanone, 2-methyl-3-(1-methylethyl)-	−2.414	97.492	1.381	0.573	No	No	No
9	1-methylcycloheptanol	−1.308	93.941	1.472	0.162	No	No	No
10	1,2,3-propanetriol	0.881	74.246	1.073	−0.362	No	No	No

No	Compound name	Water solubility (log mol/L)	Human intesntinal absorption (% Absorbed)	Caco-2 permeability (log Papp in 10^{-6} cm/s)	BBB permeability (log BB)	CYP2D6 substrate	CYP2D6 inhibitor	OCT2 substrate
11	2-decenal, (e)-	−4.125	94.9	1.491	0.695	No	No	No
12	6-methyl-6-nitro-2-heptanone	−1.921	96.918	1.29	−0.195	No	No	No
13	Isosorbide	−0.916	86.251	1.056	−0.241	No	No	No
14	2-Benzofuranmethanol, 2,4,5,6,7,7a-hexahydro-4,4,7a-trimethyl-, cis-	−2.358	95.151	1.6	0.304	No	No	No
15	Phenol, 2,6-dimethoxy-	−1.4	93.789	1.734	−0.204	No	No	No
16	8-hydroxygeraniol	−1.168	92.334	1.511	−0.057	No	No	No
17	2(4H)-Benzofuranone, 5,6,7,7a-tetrahydro-4,4,7a-trimethyl-	−2.38	97.255	1.618	0.286	No	No	No
18	1,2,3,4-tetrahydroxybutane	−0.005	61.776	0.429	−0.983	No	No	No
19	Tetradecanoic acid	−4.952	92.691	1.56	−0.027	No	No	No
20	Hexadecanoic acid, methyl ester	−6.927	92.335	1.6	0.749	No	No	No
21	Aphthosin	−3.414	80.108	−0.133	−1.966	No	No	No
22	Hexadecanoic acid	−6.927	92.335	1.6	0.749	No	No	No

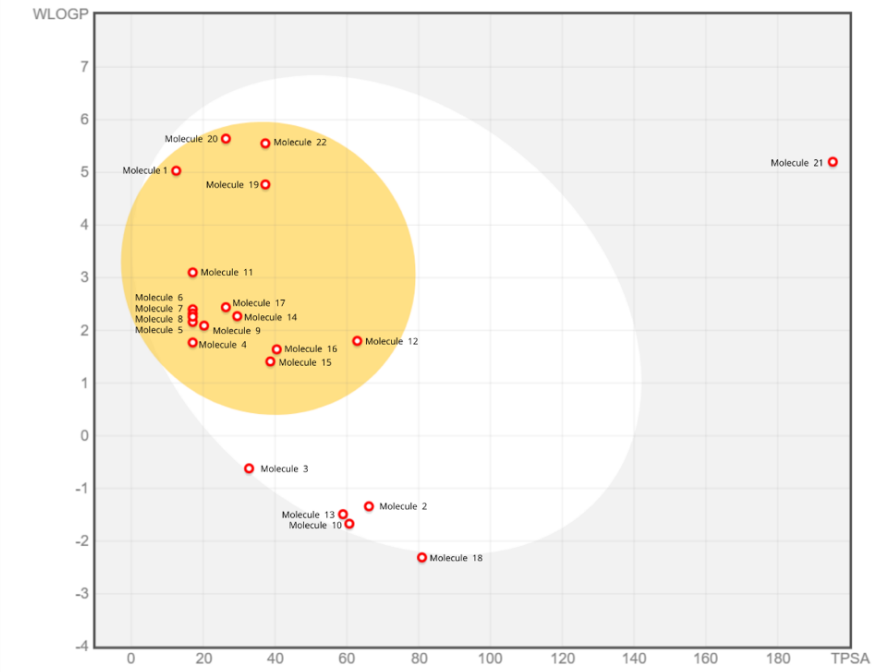

Figure 4 Prediction of brain and intestinal permeability of nanoherbal *T. aurea* components using the BOILED-Egg predictive model. White regions indicate HIA (human intestinal absorption), while yellow regions represent BBB (blood-brain barrier) permeability. The molecular order corresponds to **Table 4**.

Based on **Figure 4**, the BOILED-Egg predictive model revealed the permeability potential of *T. aurea* components across the BBB and HIA. Molecules such as Morpholine, 2,6-dimethyl-4-tridecyl-, 2-decenal, E-,

Tetradecanoic acid, and Hexadecanoic acid demonstrated strong BBB permeability due to their high lipophilicity and low TPSA values, making them promising candidates for central nervous system-targeted therapies. In contrast, molecules like Carbamic acid, monoammonium salt, 1,2,3-propanetriol, Isosorbide and 1,2,3,4-tetrahydroxybutane showed favorable intestinal absorption, indicating potential for oral bioavailability. Aphthosin exhibited limited permeability due to its high TPSA, restricting its transport across biological barriers. Meanwhile, molecules Heptanal, Cyclohexanone, 2,2,6-trimethyl-, Cyclopentanone, 2-methyl-3-(1-methylethyl)-, 1-methylcycloheptanol and Phenol, 2,6-dimethoxy- occupied regions near the BBB-HIA boundary, suggesting the need for further pharmacokinetic and bioavailability assessments to confirm their potential as therapeutic agents.

Toxicity prediction

The data presented in **Table 6**, provide a predictive toxicity profile of 22 compounds derived from *T. aurea* based on their LD50 values, predicted toxicity classes, and associated accuracy. Several compounds, such as Morpholine, 2,6-dimethyl-4-tridecyl- and Hexanal, fall into toxicity class 5, indicating they are "possibly hazardous" but are generally less toxic compared to compounds in lower toxicity classes. For instance, 1,2,3-propanetriol and Hexadecanoic acid, methyl ester also belongs to this class with relatively high LD50 values (4,090 - 5,000 mg/kg). Compounds like Carbamic acid, monoammonium salt, Oxiranemethanol, and Cyclohexanone, 2,2,6-trimethyl- are classified as toxicity class 4, indicating they are "harmful" if ingested, with LD50 values ranging from 420 to 958 mg/kg. These results suggest moderate acute toxicity. In contrast, Cyclopentanone, 2-methyl-3-(1-methylethyl)- and 2(4H)-Benzofuranone, 5,6,7,7a-tetrahydro-4,4,7a-trimethyl- are predicted to belong to toxicity class 2, indicating they are "fatal if swallowed" due to their very low LD50 values (25 and 34 mg/kg, respectively). These compounds pose a significantly higher risk of acute toxicity compared to others. Notably, 1-methylcycloheptanol and 1,2,3,4-tetrahydroxybutane are anticipated to exhibit low toxicity, with LD50 values of 7,200 and 23,000 mg/kg, respectively, categorizing them in toxicity class 6 ("non-toxic"). The prediction accuracy and similarity scores for most compounds are high, indicating reliable toxicity classifications. However, some compounds, such as 6-methyl-6-nitro-2-heptanone and Aphthosin, exhibit lower prediction accuracy (67.38% and 70.97%, respectively), which may warrant further experimental validation. This analysis highlights the diversity in toxicological profiles of compounds from *T. aurea*, ranging from non-toxic to highly toxic, emphasizing the importance of careful evaluation when considering their potential applications.

Table 6 Predicted toxicology levels of the compounds *T. aurea*.

No	Compound name	Predicted LD50 (mg/kg)	Predicted toxicity class	Average similarity	Prediction accuracy
1	Morpholine, 2,6-dimethyl-4-tridecyl-	650	5 (possibly hazardous)	100%	100%
2	Carbamic acid, monoammonium salt	681	4 (harmful)	100%	100%
3	Oxiranemethanol	420	4 (harmful)	100%	100%
4	Hexanal	3,240	5 (possibly hazardous)	100%	100%
5	Heptanal	5,000	5 (possibly hazardous)	100%	100%
6	Cyclohexanone, 2,2,6-trimethyl-	500	4 (harmful)	100%	100%
7	2 octenal	5,000	5 (possibly hazardous)	95.45%	72.9%
8	Cyclopentanone, 2-methyl-3-(1-methylethyl)-	25	2 (fatal if swallowed)	100%	100%

No	Compound name	Predicted LD50 (mg/kg)	Predicted toxicity class	Average similarity	Prediction accuracy
9	1-methylcycloheptanol	7,200	6 (non-toxic)	92.31%	72.9%
10	1,2,3-propanetriol	4,090	5 (possibly hazardous)	100%	100%
11	2-decenal, (e)-	5,000	5 (possibly hazardous)	100%	100%
12	6-methyl-6-nitro-2-heptanone	958	4 (harmful)	51.49%	67.38%
13	Isosorbide	289	3 (toxic if swallowed)	100%	100%
14	2-Benzofuranmethanol, 2,4,5,6,7,7a-hexahydro-4,4,7a-trimethyl-, cis-	4,300	5 (possibly hazardous)	67.34%	68.07%
15	Phenol, 2,6-dimethoxy-	550	4 (harmful)	100%	100%
16	8-hydroxygeraniol	2,100	5 (possibly hazardous)	95.45%	72.9%
17	2(4H)-Benzofuranone, 5,6,7,7a-tetrahydro-4,4,7a-trimethyl-	34	2 (fatal if swallowed)	85.4%	70.97%
18	1,2,3,4-tetrahydroxybutane	23,000	6 (non-toxic)	100%	100%
19	Tetradecanoic acid	900	4 (harmful)	100%	100%
20	Hexadecanoic acid, methyl ester	5,000	5 (possibly hazardous)	100%	100%
21	Aphthosin	962	4 (harmful)	82.15%	70.97%
22	Hexadecanoic acid	900	4 (harmful)	100%	100%

The data presented in **Table 7** provide a predictive organ toxicity profile of 22 compounds derived from *T. aurea*. Most compounds are predicted to cross the blood-brain barrier (BBB), as indicated by their "Active" status for this parameter. However, their potential toxicity to other organs, including the liver, kidneys, heart, and immune system, is largely minimal. For instance, compounds such as Hexanal, Heptanal, and 2-decenal (E)- are active in crossing the BBB but show no significant toxicity to other organs, suggesting their safety profile in terms of organ-specific toxicity. Similarly, Cyclopentanone, 2-methyl-3-(1-methylethyl)- is active in crossing the BBB without displaying hepatotoxicity, nephrotoxicity, cardiotoxicity, or immunotoxicity. Conversely, Oxiranemethanol and 6-methyl-6-nitro-2-heptanone demonstrate potential neurotoxicity and mutagenicity, respectively, despite their inactive status in causing hepatotoxicity and nephrotoxicity. Such findings highlight their potential risks despite limited toxicity in other areas. Compounds like Phenol, 2,6-dimethoxy- and Aphthosin are noteworthy for their nephrotoxicity while being inactive across other toxicity categories. These findings underscore the importance of evaluating kidney-specific effects in applications involving these compounds. Interestingly, 1,2,3,4-tetrahydroxybutane, a compound predicted to be non-toxic in **Table 7**, demonstrates potential nephrotoxicity and cardiotoxicity, suggesting that even compounds classified as "non-toxic" based on LD50 values might pose risks to specific organs. Overall, this analysis highlights the variability in toxicity profiles among *T. aurea* compounds, with a focus on their ability to cross the BBB and the potential risks to vital organs, underscoring the need for careful evaluation in therapeutic applications.

Table 7 Predicted organ toxicity of the compounds *T. aurea*.

No	Compound name	Organ toxicity						
		Hepato toxicity	**Neurot oxicity**	**Nephrot oxicity**	**Cardio toxicity**	**BBB barrier**	**Immuno toxicity**	**Mutageni city**
1	Morpholine, 2,6-dimethyl-4-tridecyl-	Inactive	Active	Inactive	Inactive	Active	Inactive	Inactive
2	Carbamic acid, monoammonium salt	Inactive	Inactive	Inactive	Inactive	Active	Inactive	Inactive
3	Oxiranemethanol	Inactive	Inactive	Inactive	Active	Active	Inactive	Active
4	Hexanal	Inactive	Inactive	Inactive	Inactive	Active	Inactive	Inactive
5	Heptanal	Inactive	Inactive	Inactive	Inactive	Active	Inactive	Inactive
6	Cyclohexanone, 2,2,6-trimethyl-	Inactive	Active	Inactive	Inactive	Active	Inactive	Inactive
7	2 octenal	Inactive	Inactive	Inactive	Inactive	Active	Inactive	Inactive
8	Cyclopentanone, 2-methyl-3-(1-methylethyl)-	Inactive	Inactive	Inactive	Inactive	Active	Inactive	Inactive
9	1-methylcycloheptanol	Inactive	Inactive	Inactive	Inactive	Active	Inactive	Inactive
10	1,2,3-propanetriol	Inactive	Inactive	Active	Active	Inactive	Inactive	Inactive
11	2-decenal, (e)-	Inactive	Inactive	Inactive	Inactive	Active	Inactive	Inactive
12	6-methyl-6-nitro-2-heptanone	Inactive	Inactive	Inactive	Inactive	Active	Inactive	Active
13	Isosorbide	Inactive	Inactive	Inactive	Active	Active	Inactive	Inactive
14	2-Benzofuranmethanol, 2,4,5,6,7,7a-hexahydro-4,4,7a-trimethyl-, cis-	Inactive	Inactive	Inactive	Inactive	Active	Inactive	Inactive
15	Phenol, 2,6-dimethoxy-	Inactive	Inactive	Active	Inactive	Active	Inactive	Inactive
16	8-hydroxygeraniol	Inactive	Inactive	Inactive	Inactive	Active	Inactive	Inactive
17	2(4H)-Benzofuranone, 5,6,7,7a-tetrahydro-4,4,7a-trimethyl-	Inactive	Inactive	Inactive	Inactive	Active	Inactive	Inactive
18	1,2,3,4-tetrahydroxybutane	Inactive	Inactive	Active	Active	Inactive	Inactive	Inactive
19	Tetradecanoic acid	Inactive	Inactive	Inactive	Inactive	Active	Inactive	Inactive
20	Hexadecanoic acid, methyl ester	Inactive	Inactive	Inactive	Inactive	Active	Inactive	Inactive
21	Aphthosin	Inactive	Inactive	Active	Inactive	Active	Inactive	Inactive
22	Hexadecanoic acid	Inactive	Inactive	Inactive	Inactive	Active	Inactive	Inactive

Molecular interactions of *T. aurea* compounds with 6KZZ protein

Twenty-three bioactive compounds from *T. aurea* were evaluated for their binding potential with the 6KZZ protein through molecular docking studies (**Table 8**), revealing diverse affinities that highlight their potential for antimicrobial applications. Aphthosin exhibits the greatest binding affinity among the evaluated compounds, with a binding energy of −7.4 kcal/mol, exceeding that of the control. It forms hydrogen bonds with HIS 55, ARG 76, and THR 163, while also exhibiting significant hydrophobic interactions with ILE 60 and LYS 162, indicating its relatively strong potential as an antimicrobial agent. The control compound, 4-[[8-(methylamino)-2-oxidanylidene-1H-quinolin-3-yl]carbonylamino]benzoic acid, demonstrated a robust binding energy of −6.2 kcal/mol. It interacts with residues HIS 55, ASP 74, and ARG 136 through hydrogen bonds, while also engaging with THR 163 via hydrophobic interactions. This suggests a robust interaction profile, enhancing its biological efficacy. The 3-dimensional interactions between the ligands and the 6KZZ protein are depicted in **Figures 5** and **6**, further supporting their binding profiles.

Table 8 Residue and biding energy of ligand and 6KZZ interaction.

No	Ligands	Interaction Type					Binding Afinity
		Hydrogen Bond		Hydrophobic	Electrostatis	Unfavorable	
		Hydrogen Bond	Carbon Hydrogen Bond				
		Control					
1	4-[[8-(methylamino)-2-oxidanylidene-1~{H}-quinolin-3-yl]carbonylamino]benzoic acid9 (Control)	HIS 55, ASP 74, ARG 136	THR 163	LYS 57, ARG 76	-	-	−6.2
		Bioactive components of the *T. aurea*					
1	Morpholine, 2,6-dimethyl-4-tridecyl-	-	-	ILE 60, LYS 162, ARG 204, HIS 215	-	-	−4.3
2	Carbamic acid, monoammonium salt	GLN 135, THR 163	GLY 164	-	-	GLN 72	−2.8
3	Oxiranemethanol	THR 62, SER 70		-	-	-	−2.9
4	Hexanal	ARG 76	-	-	-	-	−3.0
5	Heptanal	ARG 76			-	-	−4.2
6	Cyclohexanone, 2,2,6-trimethyl-	THR 62, SER 70	-	ILE 60, MET 166, LYS 208	-	-	−3.5
7	2 octenal	THR 163	-	ILE 60, LYS 162	-	-	−4.1
8	Cyclopentanone, 2-methyl-3-(1-methylethyl)-		-	-	-	-	−4.1
9	1-methylcycloheptanol	GLN 135	-	LYS 162	-	-	−4.1
10	1,2,3-propanetriol	ASP 49, GLU 50	ASN 46	-	-	-	−3.3
11	2-decenal, (e)-	THR 163	-	ILE 60, LYS 162	-	-	−3.6
12	6-methyl-6-nitro-2-heptanone	THR 62, SER 70, ARG 206, LYS 208	-	-	-	-	−4.2
13	Isosorbide	THR 62, SER 70	-	-	-	-	−4.0
14	2-Benzofuranmethanol, 2,4,5,6,7,7a-hexahydro-4,4,7a-trimethyl-, cis-	ASP 73	-	LYS 162	-	GLN 72	−4.8
15	Phenol, 2,6-dimethoxy-	THR 62, SER 70	-	ILE 60, HIS 64, MET 166	-	-	−4.2
16	8-hydroxygeraniol	GLY 75, THR 163	-	HIS 55, ARG 76, ARG 136	-	-	−4.4
17	2(4H)-Benzofuranone, 5,6,7,7a-tetrahydro-4,4,7a-trimethyl-	GLU 50	-	ILE 94	-	-	−4.9
18	1,2,3,4-tetrahydroxybutane	ASN 46, ASP 49, ARG 76	-	-	-	GLU 50	−3.9

No	Ligands	Interaction Type					Binding Afinity
		Hydrogen Bond		Hydrophobic	Electrostatis	Unfavorable	
		Hydrogen Bond	Carbon Hydrogen Bond				
19	Tetradecanoic acid	ARG 204	-	ILE 60, LYS 162	-	-	−4.0
20	Hexadecanoic acid, methyl ester	ARG 204	-	ILE 60, LYS 162	-	-	−4.2
21	Aphthosin	HIS 55, ARG 76, THR 163	GLU 58	ILE 60, LYS 162	-	ASP 74	−7.4
22	Hexadecanoic acid	ARG 204, ARG 206	-	LYS 162	-	-	−4.2

In contrast, numerous compounds demonstrate diminished binding affinities. The carbamic acid monoammonium salt exhibits a binding energy of −2.8 kcal/mol, forming hydrogen bonds with GLN 135 and THR 163, while lacking significant hydrophobic or electrostatic interactions. Similarly, hexanal, with a binding energy of −3.0 kcal/mol, interacts weakly with ARG 76, reflecting its limited potential in terms of biological activity. Additional compounds, including 1,2,3-propanetriol and 2-decenal, exhibit reduced binding energies of −3.3 and −3.6 kcal/mol, respectively. Their interactions are primarily based on hydrogen bonds, with minimal hydrophobic or electrostatic engagement, suggesting that these compounds may require further optimization to enhance their binding affinities and antimicrobial potential. Overall, this analysis underscores the varied interaction profiles of the bioactive compounds from *T. aurea*, highlighting both high-affinity candidates for further development and those that may benefit from structural modifications to improve their biological activity.

Protein 6KZZ, also known as *E. coli* DNA Gyrase B, is a critical enzyme in bacterial DNA replication, transcription, and repair. It is important for inserting negative supercoils into DNA to release tension during strand unwinding DNA Gyrase B is essential in the ATP-dependent strand passing mechanism, and inhibitors that target this subunit can decrease its function by attaching to the ATP-binding domain, inhibiting ATP hydrolysis and disrupting the supercoiling process. Because of its interference with DNA replication, DNA Gyrase B is an important target for antimicrobial medicines, particularly those focused at tackling resistant bacterial strains [13,27].

The agreement between the *in vitro* antibacterial activity of *T. aurea* extract particularly its inhibition of *S. aureus* and *S. Typhii* and the *in silico* docking results, where Aphthosin exhibited the most favorable binding affinity to DNA gyrase (6KZZ), suggests a potential relationship between experimental and computational findings. These results indicate that bioactive compounds from *T. aurea* may serve as promising candidates for further investigation as natural antibacterial agents targeting bacterial DNA gyrase.

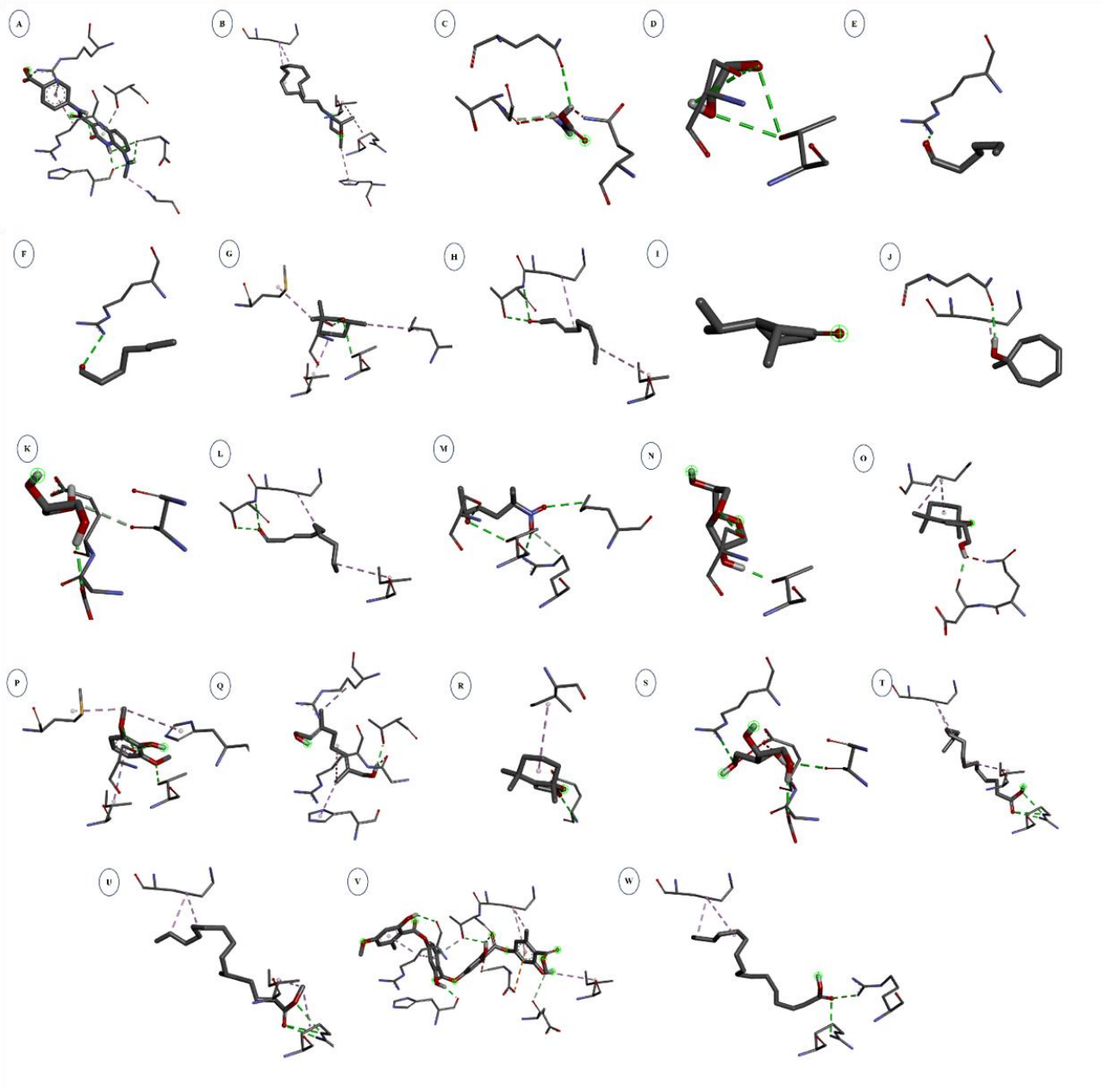

Figure 5 3D interactions of 4-[[8-(methylamino)-2-oxidanylidene-1~{H}-quinolin-3-yl]carbonylamino]benzoic acid9 and bioactive compounds from T. aurea (Linnaeus) C.Martius against the 6KZZ protein. (A) 4-[[8-(methylamino)-2-oxidanylidene-1~{H}-quinolin-3-yl]carbonylamino]benzoic acid9; (B) Morpholine, 2,6-dimethyl-4-tridecyl-, (z)-; (C) Carbamic acid, monoammonium salt; (D) Oxiranemethanol; (E) Hexanal; (F) Heptanal; (G) Cyclohexanone, 2,2,6-trimethyl-; (H) Cyclohexanol, 3,5-dimethyl-; (I) 2 octenal; (J) Cyclopentanone, 2-methyl-3-(1-methylethyl)-; (K) 1-methylcycloheptanol; (L) 1,2,3-propanetriol; (M) 2-decenal, (e)-; 6-methyl-6-nitro-2-heptanone; (O) Isosorbide; (P) 2-Benzofuranmethanol, 2,4,5,6,7,7a-hexahydro-4,4,7a-trimethyl-, cis-; (Q) Phenol, 2,6-dimethoxy; (R) 8-hydroxygeraniol; (S) 2(4H)-Benzofuranone, 5,6,7,7a-tetrahydro-4,4,7a-trimethyl-; (T) 1,2,3,4-tetrahydroxybutane; (U) Tetradecanoic acid (V) Hexadecanoic acid, methyl ester (X) Aphthosin; (Y) Hexadecanoic acid.

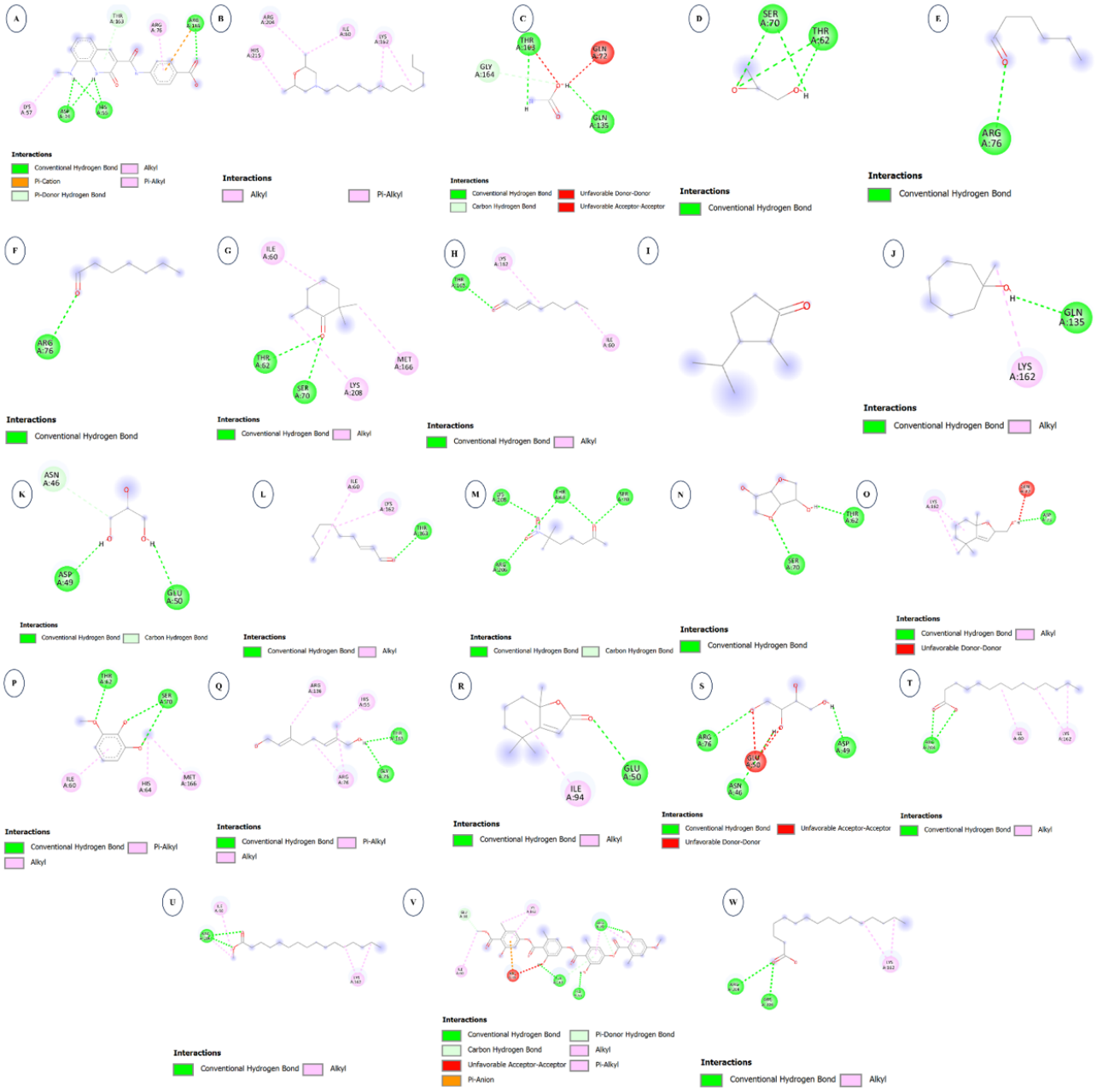

Figure 6 2D interactions of 4-[[8-(methylamino)-2-oxidanylidene-1~{H}-quinolin-3-yl]carbonylamino]benzoic acid9 (Control) and bioactive compounds from T. aurea (Linnaeus) C.Martius against the 6KZZ protein. (A) 4-[[8-(methylamino)-2-oxidanylidene-1~{H}-quinolin-3-yl]carbonylamino]benzoic acid9; (B) Morpholine, 2,6-dimethyl-4-tridecyl-, (z)-; (C) Carbamic acid, monoammonium salt; (D) Oxiranemethanol; (E) Hexanal; (F) Heptanal; (G) Cyclohexanone, 2,2,6-trimethyl-; (H) Cyclohexanol, 3,5-dimethyl-; (I) 2 octenal; (J) Cyclopentanone, 2-methyl-3-(1-methylethyl)-; (K) 1-methylcycloheptanol; (L) 1,2,3-propanetriol; (M) 2-decenal, (e)-; 6-methyl-6-nitro-2-heptanone; (O) Isosorbide; (P) 2-Benzofuranmethanol, 2,4,5,6,7,7a-hexahydro-4,4,7a-trimethyl-, cis-; (Q) Phenol, 2,6-dimethoxy; (R) 8-hydroxygeraniol; (S) 2(4H)-Benzofuranone, 5,6,7,7a-tetrahydro-4,4,7a-trimethyl-; (T) 1,2,3,4-tetrahydroxybutane; (U) Tetradecanoic acid (V) Hexadecanoic acid, methyl ester (X) Aphthosin; (Y) Hexadecanoic acid.

Conclusions

This study demonstrates that *Trentepohlia aurea* possesses antibacterial potential, particularly against Gram-positive bacteria, and contains multiple bioactive constituents as revealed by GC-MS analysis. Among these, Aphthosin emerged as a promising candidate in molecular docking studies, showing strong predicted affinity for bacterial DNA gyrase (6KZZ). While these findings suggest a possible mechanism of action and support the value of *T. aurea* as a source of natural antibacterial agents, they remain preliminary. The absence of compound isolation, direct antibacterial testing of individual constituents, and determination of MIC or MBC limits the strength of causal inferences about Aphthosin's role. Future studies should incorporate targeted purification, *in vitro* validation of key compounds, and comprehensive pharmacological profiling to confirm activity and safety. Such work could pave the way for the development of novel antibacterial agents derived from this underexplored algal species.

Acknowledgements

This work was supported by Ministry of Education, Culture, Research, and Technology, Republic of Indonesia under of PMDSU Research Grant (Contract Number: 76/UN5.4.10.K/PT.01.03/KP-DPPM/2025).

Declaration of Generative AI in Scientific Writing

No generative AI tools were used in the writing of this manuscript.

CRediT Author Statement

Oky Kusuma Atni: Investigation, Methodology, Research data collection, Data analysis, and Writing original draft. **Erman Munir:** Conceptualization, Investigation, Reviewing and editing, and Corresponding author. **Nursahara Pasaribu:** Research design, Project administration, Writing reviewing, Data curation, and Editing.

References

[1] MM El-Sheekh, N Abdullah and I Ahmad. *Handbook of research on algae as a sustainable solution for food, energy, and the environment*. IGI Global, Pennsylvania, 2022.

[2] P Mallick and S Chatterjee. *Textbook of algae*. Techsar, New Delhi, India, 2024.

[3] TNBT Ibrahim, NAS Feisal, NH Kamaludin, WY Cheah, V How, A Bhatnagar and PL Show. Biological active metabolites from microalgae for healthcare and pharmaceutical industries: A comprehensive review. *Bioresource Technology* 2023; **372**, 12866.

[4] L Chen, L Zhang and T Liu. Concurrent production of carotenoids and lipid by a filamentous microalga *Trentepohlia arborum*. *Bioresource Technology* 2016; **214**, 567-573.

[5] V Dolganyuk, D Belova, O Babich, A Prosekov, S Ivanova, D Katserov and S Sukhikh. Microalgae: A promising source of valuable bioproducts. *Biomolecules* 2020; **10(8)**, 1153.

[6] N Mishra, E Gupta, P Singh and R Prasad. *Application of microalgae metabolites in food and pharmaceutical industry*. *In*: C Egbuna, AP Mishra and MR Goyal (Eds.). Preparation of phytopharmaceuticals for the management of disorders. Academic Press, London, 2023, p. 391-408.

[7] H Upadhyay, L Saini and A Chakraborty. *Trentepohlia*. *In*: N Amaresan and K Kumar (Eds.). Compendium of phytopathogenic microbes in agro-ecology: Bacteria, protozoa, algae and nematodes. Springer Nature, Cham, Switzerland, 2025, p. 681-701.

[8] S Saraphol, S Vajrodaya, E Kraichak, A Sirikhachornkit and N Sanevas. Environmental factors affecting the diversity and photosynthetic pigments of trentepohlia species in Northern Thailand's chiang dao wildlife sanctuary. *Acta Societatis Botanicorum Poloniae* 2020; **89(1)**, 1-24.

[9] R Kant, K Sarma, N Kumar, M Sharma, NC Halder, A Tyagi, D Gupta and V Malik. Biochemical profiling of chlorophylls, carotenoids, proteins and lipids of *Trentepohlia aurea* (l) c. Martius, Chlorophyta. *Egyptian Journal of Phycology* 2024; **25(1)**, 15-20.

[10] D Zhang, M Wan, EA del Rio-Chanona, J Huang, W Wang and Y Li. Vassiliadis vs. dynamic modelling of *Haematococcus pluvialis* photoinduction for astaxanthin production in both

attached and suspended photobioreactors. *Algal Research* 2016; **13**, 69-78.

[11] D Kharkongor and P Ramanujam. Antioxidant activities of 4 dominant species of Trentepohlia (Trentepohliales, Chlorophyta). *International Journal of Complementary and Alternative Medicine* 2017; **8(5)**, 00270.

[12] E Sanniyasi and PP Raj. Accumulation of antioxidant pigment canthaxanthin (B, B-carotene-4, 4'-dione) from an aero-terrestrial, filamentous green microalga *Trentepohlia* Sp. *Bioresource Technology Reports* 2024; **25**, 101803.

[13] F Ushiyama, H Amada, T Takeuchi, N Tanaka-Yamamoto, H Kanazawa, K Nakano and N Ohtake. Lead identification of 8-(methylamino)-2-oxo-1, 2-dihydroquinoline derivatives as DNA gyrase inhibitors: Hit-to-lead generation involving thermodynamic evaluation. *ACS Omega* 2020; **5(17)**, 10145-10159.

[14] S Ruan, T Chih-Han and CR Bourne. Friend or foe: Protein inhibitors of DNA gyrase. *Biology* 2024; **13(2)**, 84.

[15] M Salman, P Sharma, M Kumar, AS Ethayathulla and P Kaur. Targeting novel sites in DNA gyrase for development of anti-microbials. *Briefings in Functional Genomics* 2023; **22(2)**, 180-194.

[16] GS Bisacchi and JI Manchester. A new-class antibacterial almost. Lessons in drug discovery and development: A critical analysis of more than 50 years of effort toward ATPase inhibitors of DNA gyrase and topoisomerase IV. *ACS Infectious Diseases* 2025; **1(1)**, 4-41.

[17] J Hudzicki. Kirby-Bauer disk diffusion susceptibility test protocol. *American Society for Microbiology* 2019; **15(1)**, 1-23.

[18] OK Atni, E Munir and N Pasaribu. Diversity of bioactive compounds from *Parmotrema xanthinum* as antimicrobial potential through *in-vitro* and *in-silico* assessment. *Biodiversitas Journal of Biological Diversity* 2024; **25(11)**, 4438-4449.

[19] OK Atni, E Munir and N Pasaribu. *In-vitro* and *in-silico* study of bioactive compounds from *Coccocarpia erythroxyli* as inhibitors targeting PBP3 (6ILE) for antibacterial applications. *Trends in Sciences* 2025; **22(8)**, 10291.

[20] S Simic, M Kosanic and B Rankovic. Evaluation of *in vitro* antioxidant and antimicrobial activities of green microalgae *Trentepohlia umbrina*. *Notulae Botanicae Horti Agrobotanici Cluj-Napoca* 2012; **40(2)**, 86-91.

[21] RM Epand, C Walker, RF Epand and NA Magarvey. Molecular mechanisms of membrane targeting antibiotics. *Biochimica et Biophysica Acta (BBA)-Biomembranes* 2016; **1858(5)**, 980-987.

[22] MP Mingeot-Leclercq and JL Décout. Bacterial lipid membranes as promising targets to fight antimicrobial resistance, molecular foundations and illustration through the renewal of aminoglycoside antibiotics and emergence of amphiphilic aminoglycosides. *MedChemComm* 2016; **7(4)**, 586-611.

[23] K Chekanov. Diversity and distribution of carotenogenic algae in Europe: A review. *Marine Drugs* 2023; **21(2)**, 108.

[24] BA Jaber, KR Majeed and AG Al Hashimi. Antioxidant and antibacterial activity of β-carotene pigment extracted from *Paracoccus homiensis* strain bka7 isolated from Air of Basra, Iraq. *Annals of the Romanian Society for Cell Biology* 2021; **25(4)**, 14006-14027.

[25] CA Lipinski, F Lombardo, BW Dominy and PJ Feeney. Experimental and computational approaches to estimate solubility and permeability in drug discovery and development settings. *Advanced Drug Delivery Reviews*1997; **23(1-3)**, 3-25.

[26] G Petit, C Kornreich, X Noel, P Verbanck and S Campanella. Alcohol-related context modulates performance of social drinkers in a visual Go/No-Go task: A preliminary assessment of event-related potentials. *Plos One* 2012; **7(5)**, e37466.

[27] K Rajakumari, K Aravind, M Balamugundhan, M Jagadeesan, A Somasundaram, P Devi and P Ramasamy. Comprehensive review of DNA gyrase as enzymatic target for drug discovery and development. *European Journal of Medicinal Chemistry Reports* 2024; **12**, 100233.